

Intramolecular and Intermolecular Perturbation on Electronic State of FAD Free in Solution and Bound to Flavoproteins: FTIR Spectroscopic Study by Using the C=O Stretching Vibrations as Probes

Yasuzo Nishina^{1,*}, Kyosuke Sato², Chiaki Setoyama³, Haruhiko Tamaoki³, Retsu Miura³ and Kiyoshi Shiga⁴

¹Department of Physiology, School of Health Sciences; Departments of ²Molecular Physiology and ³Molecular Enzymology, Graduate School of Medical Sciences, Kumamoto University, Honjo, Kumamoto 860-8556; and ⁴Department of Nursing, Kyushu University of Nursing and Social Welfare, Tomio, Tamana, Kumamoto 865-0062

The intramolecular and intermolecular perturbation on the electronic state of FAD was investigated by FTIR spectroscopy by using the C=O stretching vibrations as probes in D₂O solution. Natural and artificial FADs, *i.e.* 8-CN-, 8-Cl-, 8-H-, 8-OCH₃-, and 8-NH₂-FAD labelled by 2-¹³C, ¹⁸O=C(2), or 4,10a-¹³C₂ were used for band assignments. The C(2)=O and C(4)=O stretching vibrations of oxidized FAD were shifted systematically by the substitution at the 8-position, *i.e.* the stronger the electron-donating ability (NH₂ > OCH₃ > CH₃ > H > Cl > CN) of the substituent, the lower the wavenumber region where both the C(2)=O and C(4)=O bands appear. In contrast, the C(4)=O band of anionic reduced FAD scarcely shifted. The 1,645-cm⁻¹ band containing C(2)=O stretching vibration shifted to 1,630 cm⁻¹ in the medium-chain acyl-CoA dehydrogenase (MCAD)-bound state, which can be explained by hydrogen bonds at C(2)=O of the flavin ring. The band was observed at 1,607 cm⁻¹ in the complex of MCAD with 3-thiooctanoyl-CoA. The 23 cm⁻¹ shift was explained by the charge-transfer interaction between oxidized flavin and the anionic acyl-CoA. In the case of electron-transferring flavoprotein, two bands associated with the C(4)=O stretching vibration were obtained at 1,712 and 1,686 cm⁻¹, providing evidence for the multiple conformations of the protein.

Key words: artificial flavin, electron-transferring flavoprotein, FTIR spectroscopy, hydrogen bond, medium-chain acyl-CoA dehydrogenase.

Abbreviations: CT, charge-transfer; ETF, electron-transferring flavoprotein; MCAD, medium-chain acyl-CoA dehydrogenase.

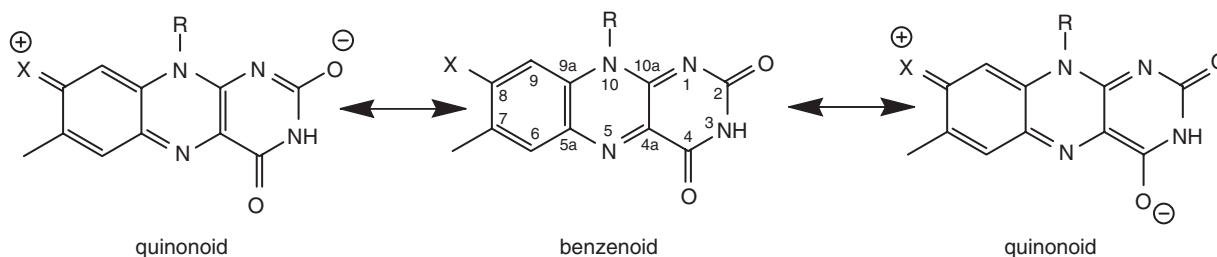
Flavins are very versatile cofactors, and flavoproteins function in various reactions including oxidation–reduction reactions. The chemical property including the reactivity of flavin molecules is governed by its electronic structure and chemical reactions in general are understood in the process defined by the generation and the destruction of chemical bonds, and the electron delocalization between reactant molecules is the source of the reaction. The delocalization is generated in the enzyme active site; thus it is important to know the perturbation on electronic state of flavin ring experienced in the active site in order to clarify the substrate and reaction specificity of flavoproteins at the molecular level; and a multitude of investigations have been carried out by various means.

Vibrational spectroscopy is one of the most useful methods for investigating molecular interactions as well as structural details. The vibration frequency obtained is a measure of the force constant between the atoms constituting a bond, and the constants are related to the bond orders and electronic distributions between

these atoms. Raman spectroscopy has been extensively employed in investigations of flavins and flavoproteins [(1) and the references cited therein]. Various Raman studies focusing on the C=O stretching vibrations of flavin have been reported (2–4). One of them is our investigation on the C(4)=O stretching mode of flavins free in solution and in some flavoproteins (3). The band derived from the C(4)=O stretching vibrational mode was assigned by isotope effects. The difference in C(4)=O frequency among flavins and flavoproteins examined was relatively large, and a linear correlation was observed between the frequency of C(4)=O stretching and the chemical shift of ¹³C(4) NMR signals (3). Recently, FTIR spectroscopy has also been successfully applied to flavins and flavoproteins, and the information on the C=O stretching vibrations has been accumulated (5–7). Iwata *et al.* (7) showed that [2-¹³C] and [4,10a-¹³C₂]flavins are useful for unequivocal assignments of the bands of the C(2)=O and C(4)=O stretching vibrations in FTIR spectra of flavoproteins.

Flavin coenzyme analogues have been used extensively as structural and mechanistic probes. Among many analogues, flavin derivatives substituted at 8 and/or 7 positions are especially valuable; the analogues systematically alter the oxidation–reduction potential of

*To whom correspondence should be addressed. Fax: +81-96-373-5490; E-mail: nishina@hs.kumamoto-u.ac.jp



Scheme 1. Resonance hybridization of oxidized flavin.

the coenzyme (8). On the basis of the shift of the Raman bands around $1,580$ and $1,540\text{ cm}^{-1}$ depending on the substituent, it was pointed out that the extent of the contribution of quinonoid form in the resonance structure (Scheme 1) is different among flavin analogues (9, 10).

In this article, we investigated the modulation of electronic state of FAD through intramolecular or intermolecular interaction by FTIR spectroscopy using the C=O stretching vibrations as probes. We discuss the electronic perturbation by the substitution at the 8-position on the basis of the band positions of the C(2)=O and C(4)=O stretching vibrations, which were assigned by using isotope-labelled natural and artificial FADs. We also obtained the bands of the C=O stretching vibrations of FAD in medium-chain acyl-CoA dehydrogenase (MCAD) and an MCAD-ligand complex, and discussed with reference to the interaction of FAD experienced in the active site. Furthermore, we obtained the bands of the C(4)=O stretching vibration of FAD in electron-transferring flavoprotein (ETF) and interpreted the results in terms of the protein conformation.

MATERIALS AND METHODS

Enzymes—MCAD was purified from porcine kidney as described by Gorelick *et al.* (11) and Lau *et al.* (12). The apoenzyme was prepared by the method of Mayer and Thorpe (13) and was reconstituted with artificial FADs following the method of Mayer and Thorpe (13) or Engst *et al.* (14). ETF was purified from porcine kidney by the method of Gorelick *et al.* (11) with some modification (15) and apoETF was prepared described elsewhere (15).

The FAD synthetase gene was amplified by the PCR method using *Corynebacterium ammoniagenes* genomic DNA as a template. *Corynebacterium ammoniagenes* was cultured in the LB medium at 30°C . The cell pellets were ground using a mortar, and suspended in 10 mM Tris, pH 8.0, 10 mM EDTA, 0.1% SDS, 20 $\mu\text{g/ml}$ RNase, 100 $\mu\text{g/ml}$ proteinase K and 2 mg/ml lysozyme. The mixture was then incubated for 1 h at 37°C . After the extraction with phenol/chloroform/isoamyl alcohol, genomic DNA was precipitated with absolute ethanol. For the amplification of the FAD synthetase gene, two primers, 5'-GATATTTGGGTACGGAACAGCAGC-3' and 5'-ATTGGCTTTTGTAGCTTTCTGCTTG-3', were synthesized, based on the published nucleotide sequence of FAD synthetase (16), which contains the 5' and 3' portions of the FAD synthetase gene, respectively. After 30 cycles of denaturation (1 min, 94°C), annealing (1 min, 62°C) and elongation (30 s, 72°C), a PCR product of

approximately 1 kb was extracted from the 1% agarose electrophoresis gel and purified. The resulting fragment was inserted into the expression vector pET-11d (Novagen) which was linearized at the unique *NcoI* site and treated with the Klenow fragment. Finally, the expression plasmid pET-FS was obtained. *Escherichia coli* BL21 (DE3) cells harbouring pET-FS were grown in 48 l of the LB medium containing 50 $\mu\text{g/ml}$ carbenicillin at 27°C for 48 h. The cells were harvested by centrifugation and stored at -20°C until use. The cell pellets were suspended in 100 mM Tris, pH 7.45, 10 mM EDTA, 1 mM DTT and treated with 0.5 mg/ml lysozyme for 1 h in an ice bath. The cells were then disrupted by sonication. FAD synthetase was prepared by the method described elsewhere (17) with some modification. The supernatant was separated by the centrifugation of homogenate containing cell debris and the fraction of 25% to 75% ammonium sulphate was collected. After dialysis against 50 mM Tris buffer pH 7.5 without NaCl, the fractions containing flavin were removed by using a Q Sepharose FAST Flow (GE Healthcare Biosciences) column ($2.5 \times 23\text{ cm}$). FAD synthetase was eluted with a 300 ml linear gradient from 0.1 to 0.3 M NaCl in 50 mM Tris buffer at pH 7.5 containing 1 mM EDTA and 1 mM DTT. The solvent of the collected flavin-free synthetase was changed to 50 mM Tris pH 7.5 and the enzyme was stored frozen at -80°C after it was concentrated with a Centriprep-30 (Millipore).

Chemicals— ^{13}C Urea (>99 atom%), $[1,3-^{13}\text{C}_2]$ diethyl malonate (>99 atom%) and D_2O (99.9 atom%) were purchased from Isotec, USA. ^{18}O Urea (97 atom%) was purchased from CEA, France. Artificial FADs were prepared from the corresponding riboflavins by the method previously reported (18). Isotope-labelled riboflavins and riboflavin analogues were prepared by using isotope-labelled barbituric acid or violuric acid. Isotope-labelled barbituric acids were synthesized from labelled urea or diethylmalonate (19) and violuric acids were prepared from barbituric acids (19). 8-NH₂-Riboflavin was prepared by a procedure described elsewhere (19,20) with the following modifications.

1-D-Ribitylamino-3-amino-4-methylbenzene (289 mg, 1.1 mmol) dissolved in 2.4 ml methanol and the solution was poured into 6 ml hot aqueous solution containing violuric acid (170 mg, 1.1 mmol) and after mixing 0.9 ml of 5% NaOH aqueous solution was added into the mixture over a period of 5 min with stirring and further stirred at 45°C for 5 min, then was left to stand in a refrigerator for several hours. The product was collected and was recrystallized from hot water. 8-CN-Riboflavin

was obtained by the procedure of Murthy *et al.* (21). 8-Cl-Riboflavin was prepared by Sandmeyer's reaction from 8-NH₂-riboflavin. 8-Demethyl-riboflavin was prepared from 8-NH₂-riboflavin by treatment of the diazo solution with phosphoric acid (22). The diazo solution of 8-NH₂-riboflavin prepared by the method described elsewhere (21) was poured into a 50% aqueous phosphinic acid cooled in an ice bath and after 1 h the mixture was poured into H₂O and was adjusted pH 6–7. The product was then purified by HPLC with a C18 column in a similar method as in 7,8-Cl₂-riboflavin purification (23). Non-labelled or isotope-labelled 8-OCH₃-riboflavin was prepared by the method described elsewhere (24) or the following method. The diazo compound of 2-methoxy-4-(1'-D-ribitylamino)-toluene (24) prepared by using aniline instead of *p*-toluidine (25) was condensed with barbituric acid by the same method for riboflavin synthesis. The molar absorption coefficients (mM⁻¹cm⁻¹) used for FAD and 8-substituted FADs are: $\epsilon_{450}(\text{FAD}) = 11.3$, $\epsilon_{450}(\text{CN}) = 11.4$, $\epsilon_{448}(\text{Cl}) = 10.6$, $\epsilon_{450}(\text{H}) = 11.3$, $\epsilon_{448}(\text{OCH}_3) = 22.0$, $\epsilon_{482}(\text{NH}_2) = 44.0$.

Spectrophotometric Measurements—Absorption spectra were measured with a Hitachi U-3310 spectrophotometer thermostated at 25°C. Visible absorption spectra of reduced FADs were obtained under anaerobic conditions by the use of a Thunberg-type cuvette. FTIR spectra were obtained by a Nicolet NEXUS 670 FTIR spectrometer. The FTIR instrument was purged with Ar gas to avoid the presence of atmospheric water vapour. Spectra were recorded at room temperature (ca. 25°C) at 4 cm⁻¹ resolution by averaging 100 scans. For FTIR measurements, the sample solution was sandwiched by CaF₂ disks, spaced with a 50 μm thick Teflon spacer. The samples were prepared in D₂O solution to avoid the interference from H₂O signal.

FTIR difference spectra between oxidized and reduced states of flavin were obtained as follows. FTIR spectra were observed before and after the photoreduction of FAD or ETF in the presence of 20 mM EDTA and then the difference spectrum was calculated with the spectrum of reduced FAD or ETF as a reference. The reduction state of the sample was confirmed by the visible absorption spectra before and after the FTIR measurements; the absorption spectra were obtained by fitting the FTIR cell in the spectrometer.

Sample Preparation for FTIR—Natural and artificial FADs were dissolved in D₂O and freeze-dried and then dissolved in a D₂O buffer solution. The flavoprotein samples for FTIR were prepared as follows. The solvent of the apoprotein solution was changed to a D₂O buffer solution by several cycles of concentration and dilution and the apoprotein was concentrated to 1–2 mM using a Centricon-30 (Millipore) centrifugation devices. The same volume of the apoprotein solution was poured into the tube containing an equimolar content of freeze-dried FADs.

RESULTS AND DISCUSSION

FTIR Difference Spectra between Non-labelled and Isotope-labelled FAD—Figure 1 shows the FTIR difference spectra of non-labelled minus [¹⁸O=C(2)]FAD (i) or

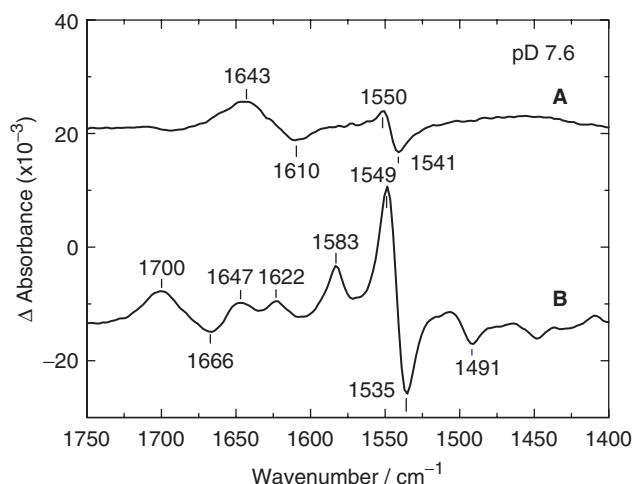


Fig. 1. FTIR difference spectra of non-labelled FAD and isotope-labelled FAD in 50 mM potassium phosphate buffer at pH 7.6. (A) Non-labelled FAD minus [¹⁸O=C(2)]FAD, (B) non-labelled FAD minus [4,10a-¹³C₂]FAD. The concentrations of FADs were 2.0 mM.

[4,10a-¹³C₂]FAD (ii) in the oxidized state in D₂O. The 1,643-cm⁻¹ band shifted to 1,610 cm⁻¹ upon [¹⁸O=C(2)]-labelling, thus being assigned to the C(2)=O stretching vibration. The Raman band of C(2)=O stretching vibration of FAD was observed at 1,676 cm⁻¹ in H₂O (4) and the corresponding band of lumiflavin in a KBr tablet was observed at 1,660 cm⁻¹ by FTIR (1). In the oxidized minus reduced FTIR difference spectra of FAD, the corresponding bands have been reported at 1,674 and 1,656 cm⁻¹ in H₂O and D₂O, respectively (5, 6). The band of the C(2)=O stretching vibration is downward-shifted by deuteration of the flavin ring, which is similar to the case of C(4)=O stretching vibration band, probably indicating that the carbonyl stretching mode also includes a contribution from N(3)-H bending (2). The bands observed at 1,550 (positive) and 1,541 (negative) cm⁻¹ correspond to the 1,547-cm⁻¹ Raman band of FAD in D₂O; this band is shifted to 1,539 cm⁻¹ upon [2-¹³C]labelling (3). Many bands exhibit isotope effects upon [4,10a-¹³C₂]labelling: 1700 (positive), 1666 (negative), 1,647 (positive), 1,622 (positive), 1,583 (positive), 1,549 (positive), 1,535 (negative) and 1,491 (negative) cm⁻¹. The 1,700-cm⁻¹ band shifted to 1,666 cm⁻¹ upon [4,10a-¹³C₂]labelling, thus being assigned to the C(4)=O stretching vibration. The C(4)=O stretching vibration of FAD was observed at 1,698 cm⁻¹ in the Raman spectrum in D₂O (3). The corresponding bands were observed at 1,708 cm⁻¹ in the FTIR difference spectra (6). These results are consistent with one another. When bands of non-labelled and isotope-labelled FADs overlap to a certain extent, the maximum difference appears at a higher frequency than the true band position, while minimum difference appears at a lower frequency than the true position. However, the deviation seems to be minimal since in the Raman spectra of FAD in D₂O solution, the 1,698- and 1,547-cm⁻¹ bands shifted to 1,664 and 1,535 cm⁻¹, respectively, upon [4,10a-¹³C₂]labelling (3). The band around 1,550 cm⁻¹ have been

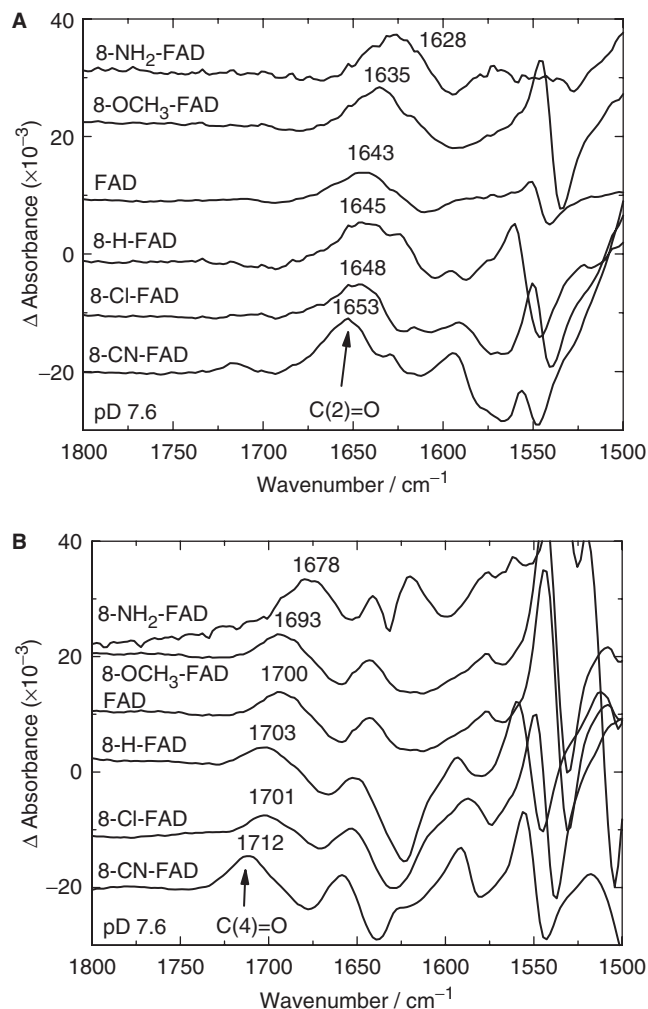


Fig. 2. FTIR difference spectra between non-labelled and isotope-labelled artificial FADs in 50 mM potassium phosphate buffer at pD 7.6. (A) Non-labelled artificial FAD minus the FAD labelled by ^{2-13}C except for natural FAD (non-labelled FAD minus $^{18}\text{O}=\text{C}(2)$ FAD). (B) Non-labelled artificial FAD minus the FAD labelled by $^{4,10\text{a}-13}\text{C}_2$. The concentrations of FADs were 2.0 mM.

assigned to the band containing the N(1)=C(10a) and C(4a)=N(5) stretchings (26).

We examined the 8-substituent effects on the C(2)=O and C(4)=O stretching vibrations of FAD (Fig. 2). The C=O bands were shifted systematically by substitution at the 8-position of FAD, *i.e.* the stronger the electron-donating ability ($\text{NH}_2 > \text{OCH}_3 > \text{CH}_3 > \text{H} > \text{Cl} > \text{CN}$) of the substituent, the lower the wavenumber region in which both C(2)=O and C(4)=O bands appear. The correlations between the band position and the Hammett σ parameter (8) are shown in Fig. 3. In the oxidized states, the substitution at the 8-position by a strong electron-donating group results in great contribution of quinonoid forms to the resonance hybridization (Scheme 1), diminishing the bond orders for C(2)=O and C(4)=O. The slopes of the least-squares fitting of the data shown in Fig. 3A and B, are similar to each other, indicating that the two quinonoid forms, *i.e.* one augmenting polarization at

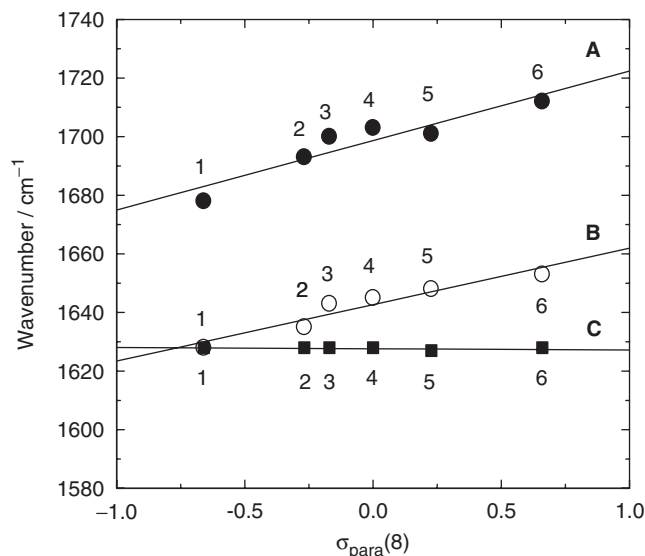


Fig. 3. Correlation between bands of C=O stretching vibrations of artificial FADs and the Hammett σ parameters for the substituents at 8-positions of the artificial FAD. Data numberings; 1, 8-NH₂-FAD; 2, 8-OCH₃-FAD; 3, FAD; 4, 8-H-FAD; 5, 8-Cl-FAD; 6, CN-FAD. The graph shows the correlation with C(4)=O stretching vibration of oxidized state (A), C(2)=O stretching vibration of oxidized form (B) or C(4)=O stretching vibration anionic reduced state (C).

C(2)=O and the other at C(4)=O, equally contribute to the polarization at these carbonyl groups.

Figure 4 shows the UV-Vis absorption spectra of natural and artificial FADs in the oxidized and reduced states. The difference in the absorption spectra of the reduced FADs at pH 5.7 and 8.3 reflects the difference in ionization state. Since the pK_a value of reduced natural FAD at N(1)-H is 6.7, the flavin moiety is mainly in the anionic and neutral states at pH 8.3 and 5.7, respectively. Although the pK_a values of artificial FADs in reduced state at N(3)-H are unknown, the conjugation is disrupted by a bend along the N(5)-N(10) axis in the reduced flavin as well as by the sp³ configurations at N(5) and N(10). Therefore, the 8-substituent effect does not propagate unto N(1)-H; the pK_a values of the reduced FADs are probably not strongly affected by 8-substituents. Thus, the reduced flavin rings may be mainly in anionic state at pD 8.5. We obtained the FTIR difference spectra of oxidized minus reduced forms in natural and artificial FADs (Fig. 5). The positive and negative bands are derived from the oxidized and reduced forms, respectively. The C(4)=O bands around 1,700 cm⁻¹ of the oxidized flavins appear at identical positions in the spectra shown in Fig. 2B. The band appearing in the 1,630–1,650 cm⁻¹ region corresponding to the C(2)=O stretching vibration disappeared upon ^{2-13}C labelling.

The negative bands around 1,630 cm⁻¹ were shifted upon $^{4,10\text{a}-13}\text{C}_2$ labelling, hence being assigned to the C(4)=O stretching vibration of anionic reduced FADs. This band is identical to those previously reported (5, 6). The corresponding band has been obtained at 1,614 cm⁻¹

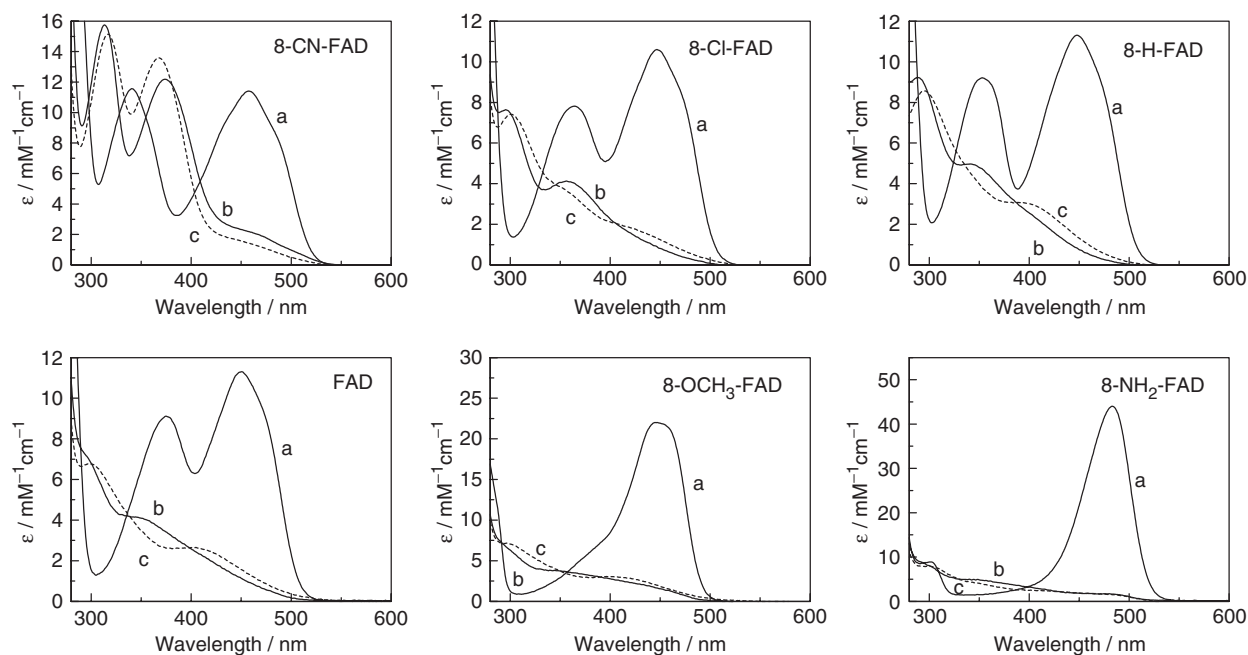


Fig. 4. **Absorption spectra of artificial FADs in the reduced FADs in a 50 mM Tris-HCl buffer at pH 8.3 (b) and oxidized and reduced states.** Spectra were measured in an anaerobic cell at 25°C. Spectra of oxidized FADs in a 50 mM potassium phosphate buffer at pH 5.7 (c). The concentrations were: FADs (14–45 μM), 50 mM potassium phosphate buffer at pH 7.6 (a), spectra of EDTA (20 mM).

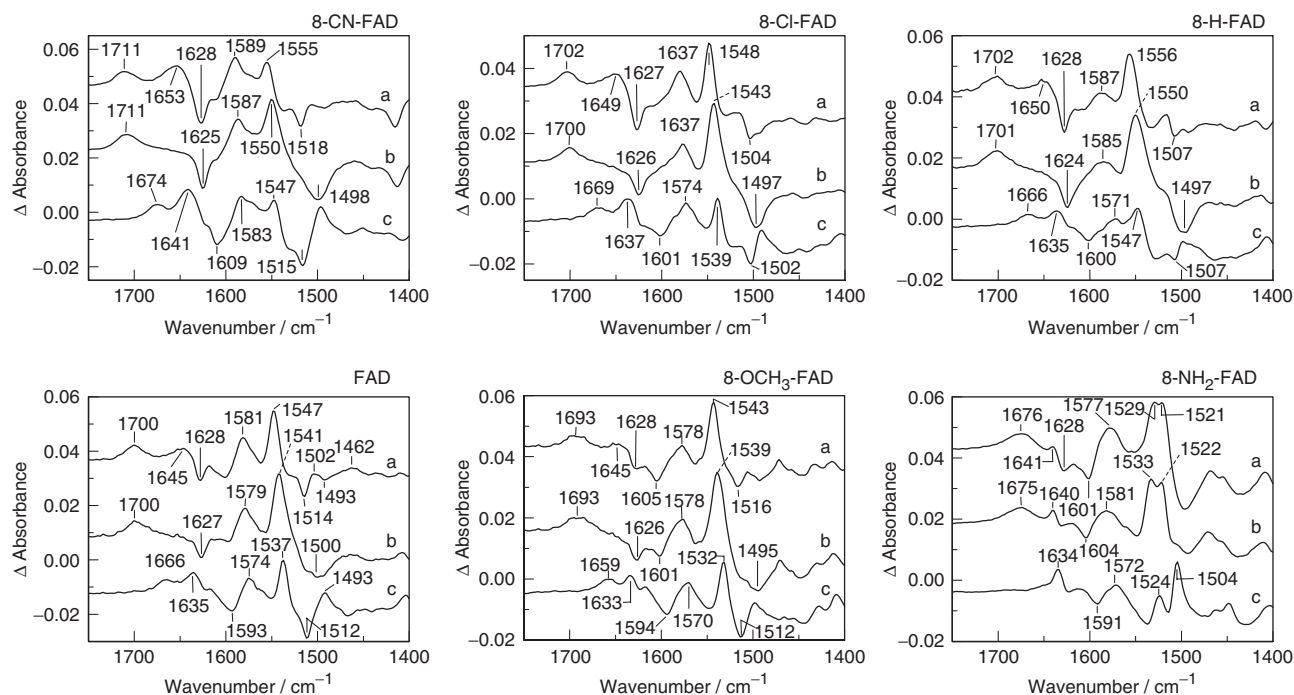


Fig. 5. **FTIR difference spectra of oxidized minus reduced forms of artificial FADs.** Spectra were obtained in a 50 mM potassium phosphate buffer at pH 8.5 containing 20 mM EDTA. (a) Non-labelled FADs; (b) $[2-^{13}\text{C}]$ FADs; (c) $[4,10a-^{13}\text{C}_2]$ FADs. The concentrations of FADs were 2 mM.

in Raman spectrum of the reduced FAD (27). The correlations between the band position and the Hammett σ parameter (8) are also shown in Fig. 3. In contrast to the case in the oxidized state, the band

of C(4)=O stretching vibration in anionic reduced flavin scarcely shifted by the substitution, indicating that the 8-substituent scarcely affects the nature of the pyrimidine moiety in reduced flavin. This can be

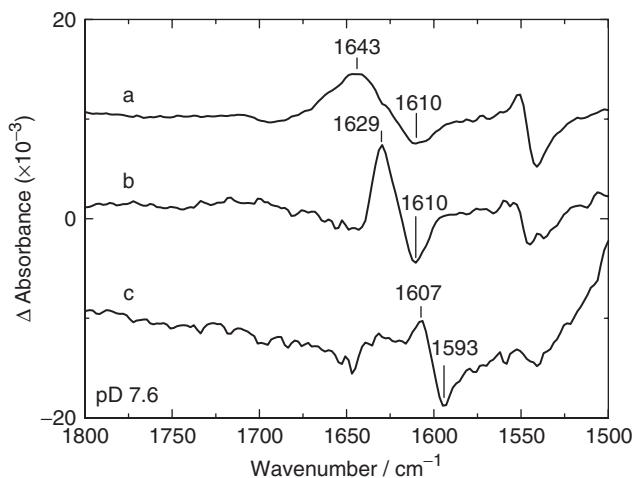


Fig. 6. FTIR difference spectra between non-labelled and [$^{18}\text{O}=\text{C}(2)$]FAD free in solution, in MCAD and in MCAD-3-thiooctanoyl-CoA complex. Spectra were obtained in a 50 mM potassium phosphate buffer at pD 7.6. (a) FAD minus [$^{18}\text{O}=\text{C}(2)$]FAD difference spectrum; (b) FAD-MCAD minus [$^{18}\text{O}=\text{C}(2)$]FAD-MCAD difference spectrum; (c) FAD-MCAD-3-thiooctanoyl-CoA complex minus [$^{18}\text{O}=\text{C}(2)$]FAD-MCAD-3-thiooctanoyl-CoA complex difference spectrum. The concentrations were: (a) FAD (2 mM); (b) FAD (1.0 mM), apoMCAD (1.4 mM); (c) FADs (1.0 mM), apoMCAD (1.4 mM), 3-thiooctanoyl-CoA (1.9 mM).

understood by the disruption of conjugation by a bend along the N(5)–N(10) axis in the reduced flavin.

MCAD—FTIR difference spectra non-labelled minus [$^{18}\text{O}=\text{C}(2)$]FADs in MCAD and MCAD-3-thiooctanoyl-CoA complex are shown in Fig. 6, and the spectrum of FAD free in solution is also shown for comparison. The 1,643- cm^{-1} band of the C(2)=O stretching vibration of FAD shifted to 1,629 and 1,607 cm^{-1} in MCAD and MCAD-3-thiooctanoyl-CoA complex, respectively. The bandwidth of the stretching absorption band of FAD bound to MCAD is narrow, compared to those of FAD free in solution. The narrowness suggests that the hydrogen bonds at C(2)=O of FAD are more rigid in enzyme bound form than those free in aqueous solution. The low frequency shift (14 cm^{-1}) in the case of MCAD is mainly explained by the hydrogen-bonding interactions at the C(2)=O group in the active site in comparison with that in aqueous solution; the group forms strong hydrogen bonds with the backbone N–H of Val135 (mean distance 3.3 Å) and Thr136 (3.2 Å) and with the hydroxyl group of Thr136 (3.1 Å) (PDB code 3MDD)(28). The 22- cm^{-1} low frequency shift upon binding of 3-thiooctanoyl-CoA cannot be explained by strengthening of hydrogen-bonding interactions at the C(2)=O moiety as the result of complex formation, because the hydrogen-bonding interaction is essentially unaltered according to the results compiled by the crystal structure of the complex (PDB code 1UDY)(29); the corresponding mean distances are 3.4, 3.3 and 3.3 Å, respectively.

The arrangement between the flavin ring and deprotonated 3-thiooctanoyl-CoA is consistent with a charge-transfer (CT) interaction with the negatively charged acyl-chain of 3-thiooctanoyl-CoA as an electron donor

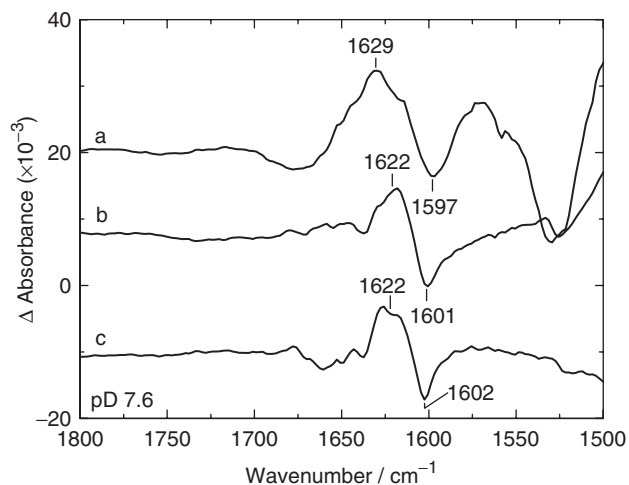


Fig. 7. FTIR difference spectra between non-labelled and [$^{18}\text{O}=\text{C}(2)$]8-NH₂-FAD free in solution, in 8-NH₂-FAD-MCAD, and 8-NH₂-FAD-MCAD-octanoyl-CoA complex. Spectra were obtained in a 50 mM potassium phosphate buffer at pD 7.6. (a) 8-NH₂-FAD minus [$^{18}\text{O}=\text{C}(2)$]8-NH₂-FAD difference spectrum; (b) 8-NH₂-FAD-MCAD minus [$^{18}\text{O}=\text{C}(2)$]8-NH₂-FAD-MCAD difference spectrum; (c) 8-NH₂-FAD-MCAD-octanoyl-CoA complex minus [$^{18}\text{O}=\text{C}(2)$]8-NH₂-FAD-MCAD-octanoyl-CoA complex difference spectrum. The concentrations were: (a) 8-NH₂-FAD (2 mM); (b) 8-NH₂-FAD (1.0 mM), apoMCAD (1.4 mM); (c) 8-NH₂-FADs (1.0 mM), apoMCAD (1.4 mM), octanoyl-CoA (1.4 mM).

stacking above the pyrimidine moiety of the flavin ring as an electron acceptor (29, 30). On the basis of the analysis involving X-ray crystallography combined with density functional theory calculations, the stabilizing energy by the CT interaction as well as the position and the intensity of the CT absorption band were investigated (29, 31). We concluded that the negative charge of deprotonated 3-thiooctanoyl-CoA is delocalized to the oxidized flavin ring and that the quantity of charge transferred from the anionic ligand onto the flavin ring was estimated to be 37% of one electron (29). Thus the large low frequency can be explained by the CT interaction, since the phases of atomic orbitals at the carbon and oxygen atoms of either C(2)=O or C(4)=O in the LUMO of oxidized flavin are opposite to each other (32) and accordingly the C=O bond orders are weakened by the electron flow into the LUMO of oxidized flavin as the result of CT.

MCAD reconstituted with 8-NH₂-FAD binds substrate acyl-CoA, but does not dehydrogenate acyl-CoA (33). Thus 8-NH₂-FAD-MCAD is a highly attractive material for investigating interactions in the enzyme-substrate complex. The complex exhibits no CT absorption band in contrast to that with 3-thiooctanoyl-CoA. FTIR difference spectra between non-labelled and [$^{18}\text{O}=\text{C}(2)$]8-NH₂-FAD in MCAD or 8-NH₂-FAD-MCAD-octanoyl-CoA complex are shown in Fig. 7, and the spectrum of 8-NH₂-FAD free in solution is also shown for comparison. The 1,629- cm^{-1} band of the C(2)=O stretching vibration of 8-NH₂-FAD shifted to 1,622 cm^{-1} upon binding to MCAD, which can be explained by the hydrogen bonds at C(2)=O. The shift (7 cm^{-1}) is smaller than that (16 cm^{-1}) for natural

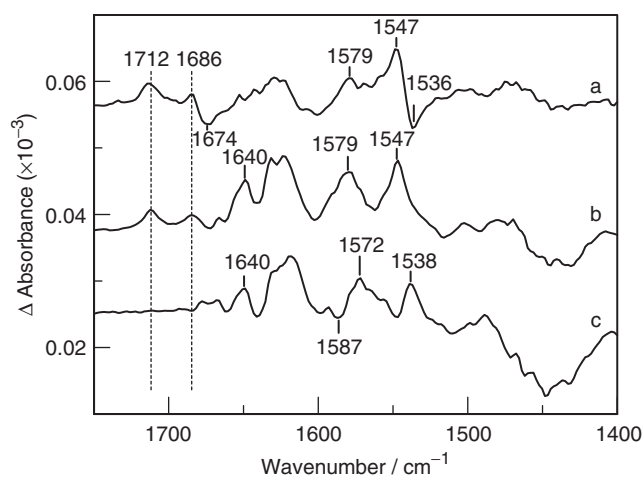


Fig. 8. FTIR difference spectra of ETF. Spectra were obtained in a 50 mM potassium phosphate buffer containing 5% glycerol and 20 mM EDTA at pD 7.6. (a) FAD-ETF minus $[4,10a\text{-}^{13}\text{C}_2]$ FAD-ETF difference spectrum in oxidized state; (b) oxidized ETF minus reduced ETF difference spectrum; (c) oxidized $[4,10a\text{-}^{13}\text{C}_2]$ FAD-ETF minus reduced $[4,10a\text{-}^{13}\text{C}_2]$ FAD-ETF. The concentrations were; FADs (0.5 mM), apoETF (0.74 mM).

FAD (Fig. 6); this may be explained by the fact that the polarization at C(2)=O is already larger in the case of 8-NH₂-FAD than natural FAD free in solution as discussed earlier. The 1,622-cm⁻¹ band does not shift by complexation of 8-NH₂-FAD-MCAD with substrate octanoyl-CoA, suggesting that hydrogen bonds at C(2)=O are not affected by the substrate binding. It is consistent with the fact that the hydrogen bonds at the C(2)=O is not affected by complexation of MCAD with 3-thiooctanoyl-CoA as discussed earlier.

Electron-transferring Flavoprotein—FTIR difference spectrum ETF reconstituted with non-labelled FAD minus ETF reconstituted with $[4,10a\text{-}^{13}\text{C}_2]$ FAD was obtained (Fig. 8, Spectrum a). This spectrum is similar to the Spectrum b in Fig. 1; positive bands appear around 1,550, 1,580 and 1,640 cm⁻¹ in both cases. The broad band from 1,620 to 1,650 cm⁻¹ (Fig. 8, Spectrum a) seems to correspond to the 1,622- and 1,647-cm⁻¹ bands of free FAD (Fig. 1, Spectrum B). But unlike FAD free in solution, two bands at 1,712 and 1,686 cm⁻¹ in the 1,700 cm⁻¹ region were observed. The 1,712-cm⁻¹ band probably shifted to 1,674 cm⁻¹ upon $[4,10a\text{-}^{13}\text{C}_2]$ labelling, since the 1,700-cm⁻¹ band shifted to 1,666 cm⁻¹ in FAD free in solution (Fig. 1, Spectrum B). The IR difference spectra of oxidized minus reduced states for ETF reconstituted with non-labelled FAD (b) and $[4,10a\text{-}^{13}\text{C}_2]$ FAD (c) are shown in Fig. 8. Both bands at 1,712 and 1,686 cm⁻¹ disappeared in the case of $[4,10a\text{-}^{13}\text{C}_2]$ FAD whereas the 1,579- and 1,547-cm⁻¹ bands for oxidized FAD bound to ETF shifted to 1,572 and 1,538 cm⁻¹, respectively. The positive bands appear around 1,620 cm⁻¹ in the Spectrum c, unlike FAD free in solution (Fig. 5, bottom left, Spectrum c). The bands may be associated with structural perturbation of the apoenzyme caused by photoreduction of FAD. The 1,640-cm⁻¹ (in the region from 1,645 to 1,653 cm⁻¹) band obtained in

Spectra b and c may also be derived from the apoenzyme, because if the band were associated with the C(2)=O stretching vibration of oxidized FAD bound to ETF, the band would have to be downward shifted by ca. 10 cm⁻¹ upon $[4,10a\text{-}^{13}\text{C}_2]$ labelling (Fig. 5, bottom left). These results provide compelling evidence that isotope-labelled compounds are important for band assignments. The band for C(4)=O stretching vibration of reduced FAD expected to appear around 1,630 cm⁻¹ was not obtained; the band is probably concealed behind the positive bands. However, the 1,587-cm⁻¹ band for reduced ETF reconstituted with $[4,10a\text{-}^{13}\text{C}_2]$ FAD may correspond to the 1,593-cm⁻¹ band of the C(4)=O band for reduced FAD free in solution (compare Spectrum c, Fig. 8 and Spectrum c, bottom left, Fig. 5).

Recently, Raman spectroscopic study on methylotrophic bacterium W3A1 ETF (wETF) was reported by Yang and Swenson (4). They obtained an unusually high frequency band (1,731 cm⁻¹) for the C(4)=O stretching vibration of FAD in wETF in H₂O; the corresponding band of FAD free in solution being observed at 1,706 cm⁻¹. From X-ray crystallographic study, several heteroatoms are within 3.5 Å of C(4)=O, including the backbone N-H of αSer254 (3.0 Å) and Gln253 (3.2 Å), and the hydroxyl group of Ser254 (3.0 Å) (PDB code, 1O97)(34). The high frequency of the Raman band suggests that hydrogen-bonding interactions with C(4)=O are very weak or non-existent and they argued that the flavin environment may not favour the formation of strong hydrogen bonds with C(4)=O in wETF. They also referred to the possibility that the frequency of the carbonyl may be influenced by unfavourable dipolar interactions. Based on the structures of free human ETF (PDB code 1EFV) (35) and wETF (PDB code 1O97), it was proposed that human wild-type ETF exists in solution as an ensemble of two interconverting states (36). In the present case of porcine ETF, two bands of C(4)=O stretching vibration were observed at 1,712 and 1,686 cm⁻¹, indicating multiple conformations of the ETF, i.e. one with strong hydrogen-bond(s), and the other with weak hydrogen-bond(s) at C(4)=O. The 3D structure of porcine ETF being unavailable at present, the mechanistic implications of multiple conformations deduced herein should be interpreted by integrating FTIR observations with the 3D structure of porcine ETF both in the absence and presence of an electron-transfer partner in complex with it.

REFERENCES

1. Nishina, Y., Sato, K., Miura, R., Matsui, K., and Shiga, K. (1998) Resonance Raman study on reduced flavin in purple intermediate of flavoenzyme: use of $[4\text{-carbonyl-}^{18}\text{O}]$ -enriched flavin. *J. Biochem.* **124**, 200–208
2. Kim, M. and Carey, P.C. (1993) Observation of a carbonyl feature for riboflavin bound to riboflavin binding protein in red-excited Raman spectrum. *J. Am. Chem. Soc.* **115**, 7015–7016
3. Hazekawa, I., Nishina, Y., Sato, K., Shichiri, M., Miura, R., and Shiga, K. (1997) A Raman study on the C(4)=O stretching mode of flavins in flavoenzymes: hydrogen bonding at the C(4)=O moiety. *J. Biochem.* **121**, 1147–1154
4. Yang, K.-Y. and Swenson, R. P. (2007) Nonresonance Raman study of the flavin cofactor and its interactions in

- the Methylotrophic Bacterium W3A1 electron-transfer flavoprotein. *Biochemistry* **46**, 2298–2305
5. Hellwig, P., Scheide, D., Bungert, S., Maentele, W., and Friedrich, T. (2000) FT-IR spectroscopic characterization of NADH: ubiquinone oxidoreductase (complex I) from *Escherichia coli*: oxidation of FeS cluster N2 is coupled with the protonation of an aspartate or glutamate side chain. *Biochemistry* **39**, 10884–10891
 6. Wille, G., Ritter, M., Friedemann, R., Maentele, W., and Huebner, G. (2003) Redox-triggered FTIR difference spectra of FAD in aqueous solution and bound to flavoproteins. *Biochemistry* **42**, 14814–14821
 7. Iwata, T., Nozaki, D., Sato, Y., Sato, K., Nishina, Y., Shiga, K., Tokutomi, S., and Kandori, H. (2006) Identification of the C=O stretching vibrations of FMN and peptide backbone by ¹³C-Labeling of the LOV2 domain of *Adiantum* phytochrome3. *Biochemistry* **45**, 15384–15391
 8. Edmondson, D.E. (1999) Electronic effects of 7 and 8 ring substituents as predictors of flavin oxidation-reduction potentials in *Flavins and Flavoproteins* (Ghisla, S., Kroneck, P., Macheroux, P., and Sund, H. eds.) pp. 71–76 Rudolf Weber, Berlin
 9. Nishina, Y., Shiga, K., Horiike, K., Tojo, H., Kasai, S., Yanase, K., Matsui, K., Watari, H., and Yamano, T. (1980) Vibrational modes of flavin bound to riboflavin binding protein from egg white. Resonance Raman spectra of lumiflavin and 8-substituted riboflavin. *J. Biochem.* **88**, 403–409
 10. Schopfer, L.M., Haushalter, J.P., Smith, M., Milad, M., and Morris, M.D. (1981) Resonance Raman spectra for flavin derivatives modified in the 8 position. *Biochemistry* **20**, 6734–6739
 11. Gorelick, R.J., Mizzer, J.P., and Thorpe, C. (1982) Purification and properties of electron-transferring flavoprotein from pig kidney. *Biochemistry* **21**, 6936–6942
 12. Lau, S.-M., Powell, P., Buettner, H., Ghisla, S., and Thorpe, C. (1986) Medium-chain acyl coenzyme A dehydrogenase from pig kidney has intrinsic enoyl coenzyme A hydratase activity. *Biochemistry* **25**, 4184–4189
 13. Mayer, E.J. and Thorpe, C. (1981) A method for resolution of general acyl-CoA dehydrogenase apoprotein. *Anal. Biochem.* **116**, 227–229
 14. Engst, S., Vock, P., Wang, M., Kim, J.-J., and Ghisla, S. (1999) Mechanism of activation of acyl-CoA substrates by medium chain acyl-CoA dehydrogenase: interaction of the thioester carbonyl with the flavin adenine dinucleotide ribityl side chain. *Biochemistry* **38**, 257–267
 15. Sato, K., Nishina, Y., Shiga, K., Tojo, H., and Tada, M. (1991) The existence of two different forms of apo-electron-transferring flavoprotein. *J. Biochem.* **109**, 734–740
 16. Nakagawa, S., Igarashi, A., Ohta, T., Hagihara, T., Fujio, T., and Aisaka, K. (1995) Nucleotide sequence of the FAD synthetase gene from *Corynebacterium ammoniagenes* and its expression in *Escherichia coli*. *Biosci. Biotechnol. Biochem.* **59**, 694–702
 17. Efimov, I., Kuusk, V., Zhang, X., and McIntire, W. S. (1998) Proposed steady-state kinetic mechanism for *Corynebacterium ammoniagenes* FAD synthetase produced by *Escherichia coli*. *Biochemistry* **37**, 9716–9723
 18. Nishina, Y., Sato, K., Tamaoki, H., Tanaka, T., Setoyama, C., Miura, R., and Shiga, K. (2003) Molecular mechanism of the drop in the pK_a of a substrate analog bound to medium-chain acyl-CoA dehydrogenase: implications for substrate activation. *J. Biochem.* **134**, 835–842
 19. Juri, N., Kubo, Y., Kasai, S., Otani, S., Kusunose, M., and Matsui, K. (1987) Formation of roseoflavin from 8-amino- and 8-methylamino-8-demethyl-D-riboflavin. *J. Biochem.* **101**, 705–711
 20. Berezovskii, V.M., Tul'chinskaya, L.S., and Polyakova, N.A. (1965) Allo- and isoalloxazine series. XIII. Synthesis of 7-amino-alloxazine, 7-aminodemethylriboflavine, and their derivatives. *Zh. Obshch. Khim.* **35**, 673–677
 21. Murthy, Y.V.S.N. and Massey, V. (1998) Synthesis and properties of 8-CN flavin nucleotide analogs and studies with flavoproteins. *J. Biol. Chem.* **273**, 8975–8982
 22. Robinson, M.M. and Robinson, B.L. (1963) 2,4,6-Tribromobenzoic acid in *Organic Synthesis Coll.* Vol. IV, pp. 947–950 John Wiley & Sons, Inc., NY
 23. Nishina, Y., Sato, K., Shi, R., Setoyama, C., Miura, R., and Shiga, K. (2001) On the ligands in charge-transfer complexes of porcine kidney flavoenzyme D-amino acid oxidase in three redox states: a resonance Raman study. *J. Biochem.* **130**, 637–647
 24. Kasai, S., Yamanaka, S., Wang, S.-C., and Matsui, K. (1979) Anti-riboflavin activity of 8-o-alkyl derivatives of riboflavin in some gram-positive bacteria. *J. Nutr. Sci. Vitaminol.* **25**, 289–298
 25. Ortiz-Maldonado, M., Aeschliman, S.M., Ballou, D.P., and Massey, V. (2001) Synergistic interactions of multiple mutations on catalysis during the hydroxylation reaction of p-hydroxybenzoate hydroxylase: studies of the Lys297Met, Asn300Asp, and Tyr385Phe mutants reconstituted with 8-Cl-flavin. *Biochemistry* **40**, 8705–8716
 26. Abe, M. and Kyogoku, Y. (1987) Vibrational analysis of flavin derivatives: normal coordinate treatments of lumiflavin. *Spectrochim. Acta* **43A**, 1027–1037
 27. Zeng, Y., Carey, P.R., and Palfey, B.A. (2004) Raman spectrum of fully reduced flavin. *J. Raman Spectrosc.* **35**, 521–524
 28. Kim, J.-J. P., Wang, M., and Paschke, R. (1993) Crystal structures of medium-chain acyl-CoA dehydrogenase from pig liver mitochondria with and without substrate. *Proc. Natl. Acad. Sci. USA* **90**, 7523–7527
 29. Satoh, A., Nakajima, Y., Miyahara, I., Hirotsu, K., Tanaka, T., Nishina, Y., Shiga, K., Tamaoki, H., Setoyama, C., and Miura, R. (2003) Structure of the transition state analog of medium-chain acyl-CoA dehydrogenase. Crystallographic and molecular orbital studies on the charge-transfer complex of medium-chain acyl-CoA dehydrogenase with 3-thiaoctanoyl-CoA. *J. Biochem.* **134**, 297–304
 30. Tamaoki, H., Nishina, Y., Shiga, K., and Miura, R. (1999) Mechanism for the recognition and activation of substrate in medium-chain acyl-CoA dehydrogenase. *J. Biochem.* **125**, 285–296
 31. Tanaka, T., Tamaoki, H., Nishina, Y., Shiga, K., Ohno, T., and Miura, R. (2006) Theoretical study on charge-transfer interaction between acyl-CoA dehydrogenase and 3-thiaacyl-CoA using density functional method. *J. Biochem.* **139**, 847–855
 32. Nishimoto, K., Fukunaga, H., and Yagi, K. (1986) Studies in a model system on the effect of hydrogen bonding at hetero atoms of oxidized flavin on its electron acceptability. *J. Biochem.* **100**, 1647–1653
 33. Nishina, Y., Sato, K., Tamaoki, H., Setoyama, C., Miura, R., and Shiga, K. (2005) Molecular mechanism for substrate specificity/activation of medium-chain acyl-CoA dehydrogenase: a FT-IR study in *Flavins and Flavoproteins 2005* (Nishino, T., Miura, R., Tanokura, M., and Fukui, K. eds.) pp. 227–232 ARChitect inc., Tokyo
 34. Leys, D., Basran, J., Talfournier, F., Sutcliffe, M.J., and Scrutton, N.S. (2003) Extensive conformational sampling in a ternary electron transfer complex. *Nature Struct Biol.* **10**, 219–225
 35. Roberts, D.L., Frerman, F.E., and Kim, J.-J. (1996) Three-dimensional structure of human electron transfer flavoprotein to 2.1-Å resolution. *Proc. Natl. Acad. Sci. USA* **93**, 14355–14360
 36. Toogood, H.S., van Thiel, A., Scrutton, N.S., and Leys, D. (2005) Stabilization of non-productive conformations underpins rapid electron transfer to electron-transferring flavoprotein. *J. Biol. Chem.* **280**, 30361–30366